SPANDIDOS PUBLICATIONS

INTERNATIONAL JOURNAL OF MOLECULAR MEDICINE 52: 95, 2023

# Adropin attenuates pancreatitis-associated lung injury through PPARγ phosphorylation-related macrophage polarization

FADIAN DING[1,2*], GUOZHONG LIU[1,2*], FENG GAO[3], ZHOU ZHENG[2], YUPU HONG[1,2], YOUTING CHEN[1,2] and SHANGENG WENG[1,2]

[1]Department of Hepatopancreatobiliary Surgery, [2]Institute of Abdominal Surgery and [3]Department of Pathology, The First Affiliated Hospital of Fujian Medical University, Fuzhou, Fujian 350004, P.R. China

Received June 22, 2023; Accepted August 11, 2023

DOI: 10.3892/ijmm.2023.5298

**Abstract.** Acute pancreatitis (AP)-associated lung injury (ALI) is a critical complication of AP. Adropin is a regulatory protein of immune metabolism. The present study aimed to explore the immunomodulatory effects of adropin on AP-ALI. For this purpose, serum samples of patients with AP were collected and the expression levels of serum adropin were detected using ELISA. Animal models of AP and adropin knockout (Adro-KO) were constructed, and adropin expression in serum and lung tissues was investigated. The levels of fibrosis and apoptosis were evaluated using hematoxylin and eosin staining, Masson's staining and immunohistochemistry of in lung tissue. M1/M2 type macrophages in the lungs were detected using immunofluorescence staining, western blot analysis and reverse transcription-quantitative PCR. As shown by the results, adropin expression was decreased in AP. In the Adro-KO + L-arginine (L-Arg) group, macrophage infiltration, fibrosis and apoptosis were increased. The expression of peroxisome proliferator- activated receptor γ (PPARγ) was downregulated, and the macrophages exhibited a trend towards M1 polarization in the Adro-KO + L-Arg group. Adropin exogenous supplement attenuated the levels of fibrosis and apoptosis in the model of AP. Adropin exogenous supplement also increased PPARγ expression by the regulation of the phosphorylation levels, which was associated with M2 macrophage polarization. On the whole, the findings of the present study suggest that adropin promotes the M2 polarization of lung macrophages and reduces the severity of AP-ALI by regulating the function of PPARγ through the regulation of its phosphorylation level.

*Correspondence to:* Dr Youting Chen or Professor Shangeng Weng, Department of Hepatopancreatobiliary Surgery, The First Affiliated Hospital of Fujian Medical University, 20 Cha-Zhong Road, Fuzhou, Fujian 350004, P.R. China
E-mail: chenyt1381@163.com
E-mail: shangeng@sina.com

[*]Contributed equally

*Key words:* pancreatitis-associated lung injury, adropin, macrophage polarization, PPARγ phosphorylation, apoptosis

## Introduction

Acute pancreatitis (AP) is a common exocrine inflammatory disease of the pancreas that can cause severe abdominal pain, multiple organ dysfunction, pancreatic necrosis and persistent organ failure. AP is associated with a mortality rate of 1-5% (1). However, the mortality rate of patients with severe AP is between 15 and 35% (2). Ulinastatin has been shown to attenuate lipopolysaccharide (LPS)-induced associated lung injury (ALI) by suppressing the activation of the Toll-like receptor 4/NF-κB pathway, associated with neutrophil, macrophage and myeloperoxidase activities (3). One of the potential mechanisms of ulinastatin is through the inflammatory response, whose main signaling pathways are TNF-α, and the high mobility group box 1-mediated inflammatory amplification of NF-κB and IL-6-mediated JAK2/STAT3 signaling pathway in AP-ALI (4). Melatonin has been demonstrated to exert a protective effect on AP-ALI in a rat model, possibly mediated via the upregulation of IL-22 and Th22 levels to improve the innate immunity of tissue cells and promote lung tissue regeneration (5). At present, the therapeutic efficacy of AP-ALI needs to be improved, and immune cell-related therapy may be a beneficial approach.

Adropin is a peptide hormone encoded by the energy homeostasis-associated (*Enho*) gene, composed of 76 amino acids. Adropin is mainly expressed in the liver, brain, heart, kidneys, pancreas, coronary artery, umbilical vein and other tissues, with the highest expression observed in the brain. Adropin can participate in the negative regulation of the immune system and play an anti-inflammatory role in atherosclerosis, fatty inflammation, fatty liver, non-alcoholic hepatitis, pulmonary vasculitis (6) and multiple sclerosis (7), where the level of adropin in multiple sclerosis is significantly reduced. Notably, adropin therapy has been shown to effectively reduce the monolayer migration of macrophages induced by monocyte chemotactic protein-1 regulation (8). A previous study demonstrated that the relative number of Tregs in patients with fatty pancreas and type 2 diabetes was positively associated with adropin (9). Another study also demonstrated and adropin knockout (Adro-KO) mice presented with myeloperoxidase

(MPO)-anti-neutrophil cytoplasm autoantibody-associated alveolar bleeding and abnormal Treg cell function (10).

Therefore, it was hypothesized that adropin may play a role in the immune regulation of AP-ALI. Combined with the aforementioned experimental findings, it was hypothesized that adropin may exert a protective effect against AP-ALI mediated by the regulation of macrophage phenotypes. The present study aimed to explore the protective effects of adropin on AP-ALI and its possible mechanisms of action using a combination of clinical samples and animal models.

## Materials and methods

*Clinical samples*. A total of 23 serum samples were collected from patients with AP and healthy controls between November, 2021 and January, 2022 at The First Affiliated Hospital of Fujian Medical University, Fuzhou, China. The mean age of the patients in the AP-ALI and control groups was 49.9 and 45.0 years, respectively, and the proportion of female patients was 60 and 46.2%, respectively. All patients were confirmed by lipase, amylase and imaging examinations. All patients provided informed consent for excess specimens to be used for research purposes and all protocols employed in the study were approved by the Medical Ethics Committee of The First Affiliated Hospital of Fujian Medical University [MTCA, ECFAH of FMU(2015) 084-1].

*Animal model*. The Adro-KO mice used in the present study were developed by Shanghai Southern Model Biotechnology Co., Ltd, with a genetic background of C57BL/6J. Non-homologous recombination repair induced reading frame shift mutations were introduced using CRISPR/Cas9 to generate the loss of *Enho* gene function (9) (Fig. S1). A total of 30 male KO mice, weighing 20-25 g and 8 weeks old, were used in the present study.

In addition, 48 wild-type male mice weighing 20-25 g and aged 8 weeks were purchased from the Wu's Animal Laboratory Center (http://www.wssydw.com/m/index.asp) and housed in a clean feeding environment. All the mice were kept at 24-26% temperature and 50-60% humidity, and a 12/12 h light/dark cycle, and were provided with free access to food and water. All animal experiments complied with the National Institutes of Health guidelines for the care and used of laboratory animals, and the protocol was approved by the Ethics Committee of Fujian Medical University (IACUC FJMU 2022-0428).

The mouse model of AP-ALI induced by the use of 10% L-arginine (L-Arg) was established according to a previously published protocol (11). Briefly, the male mice were intraperitoneally injected with L-Arg at 4 g/kg/time at an interval of 1 h. The animals were sacrificed at 48 h following the intraperitoneal injection of L-Arg (cat. no. A8220, Beijing Solarbio Science & Technology Co., Ltd.). The animals were anesthetized using isofluorane and euthanized by exsanguination through the inferior vena cava; the induction and maintenance concentrations were 3 and 1%, respectively. Following sacrifice, pain response, cardiac and respiratory arrest were observed to confirm euthanasia. Serum samples from the inferior vena cava were collected and pancreatic tissue samples were harvested. Pancreatic and lung tissues were stored at -80°C for protein analysis and the remaining samples were fixed in 10% formalin for pathological examination.

The mice were randomly assigned to one of the following groups: i) The WT + NS group (n=12), where the mice received an intraperitoneal injection of normal saline; ii) the WT + L-Arg group (n=12), where the mice were intraperitoneally injected with 10% L-Arg (4 mg/kg); iii) the Adro-KO + NS group (n=12), where Adro-KO transgenic mice were intraperitoneally injected with normal saline; iv) the Adro-KO + L-Arg group (n=12), where the Adro-KO transgenic mice received an intraperitoneal injection of 10% L-Arg (4 mg/kg); v) the Adro-KO + L-Arg + Adro$^{(34-76)}$ group (n=12), where the Adro-KO transgenic mice received an intraperitoneal injection of 10% L-Arg (4 mg/kg) plus adropin$^{(34-76)}$ [cat. no. 126418, GL Biochem (Shanghai) Ltd. 450 nmol/kg via intraperitoneal injection] five times (Fig. S2) (12,13).

*Hematoxylin and eosin (H&E) staining and Masson's staining*. The tissue samples were paraffin-sectioned with 4% polyformaldehyde for 24 h, and 4-$\mu$m-thick tissue slices were prepared, which were dipped in hematoxylin solution for 5-10 min, followed by placement in eosin solution for 0.5-2 min (cat. no. G1076, Wuhan Servicebio Technology Co., Ltd.) at room temperature. The sections were placed in 95% ethanol for de-hydration and placed in xylene and sealed with neutral gum. Images was obtained using a light microscope (Leica Microsystems GmbH). The pancreatic tissue sections were scored for the severity of pancreatitis based on edema, inflammation, vacuolization and necrosis. The individual scores were then added to obtain the total pathological score for the pancreatic tissue. As previously mentioned, the scales of interstitial and alveolar edema, interstitial and alveolar leukocyte infiltration and fibrosis were used to assess the extent of lung injury (14).

The tissue samples were paraffin-sectioned with 4% polyformaldehyde for 24 h and 4-$\mu$m-thick tissue slices were prepared. Masson's reagent (cat. no. G1006, Wuhan Servicebio Technology Co., Ltd.) was used as per the manufacturer's instructions at room temperature. Images was obtained using a light microscope (Leica Microsystems GmbH). Masson's staining was subsequently quantified by determining the collagen fiber area/non-collagen fiber area.

*Immunohistochemistry*. The paraffin-embedded sections were de-waxed, soaked in recovery buffer containing EDTA antigen (Wuhan Servicebio Technology Co., Ltd.), and incubated with the primary antibodies at 4°C overnight. The sections were then incubated in HRP-secondary antibody (1:200; cat. no. G1213, Wuhan Servicebio Technology Co., Ltd.) at room temperature for 2 h. Following incubation with DAB (cat. no. G1212, Wuhan Servicebio Technology Co., Ltd.) and hematoxylin (cat. no. G1004, Wuhan Servicebio Technology Co., Ltd.), the sections were sealed with neutral resin (cat. no. WG10004160, Wuhan Servicebio Technology Co., Ltd.). Images was obtained using a light microscope (Leica Microsystems GmbH). The primary antibodies used were the following: MPO (1:200, cat. no. YT5351, ImmunoWay), CD68 (1:200, cat. no. ab283654, Abcam), caspase-3 (1:200, cat. no. A0214, ABclonal), poly(ADP-ribose) polymerase 1 (PARP1; 1:200, cat. no. A19596, ABclonal) and TGF-β (1:200, cat. no. bs-0103R, BIOSS).

*Immunofluorescence*. The paraffin-embedded sections were completely dewaxed with xylene, anhydrous ethanol, 90% ethanol, 75% ethanol and 50% ethanol, and immersed in antigen repair solution, membrane breaking solution (cat. no. G1204, Wuhan Servicebio Technology Co., Ltd.), and, the sections were sealed with neutral resin (cat. no. WG10004160, Wuhan Servicebio Technology Co., Ltd.). The sections were incubated in primary antibody at 4˚C overnight, followed by incubation with goat anti-rat FITC (1:200, cat. no. BA1108, Boster Bio) and goat anti-rabbit Alexa Fluor 594 (1:200, cat. no. ASP1365, Abcepta) antibodies at room temperature for 2 h, respectively. Following incubation with DAPI (2 $\mu$g/ml; cat. no. G1012, Wuhan Servicebio Technology Co., Ltd.) at room temperature for 5 min, the sections were sealed with anti-fluorescence quenching reagent (cat. no. G1401, Wuhan Servicebio Technology Co., Ltd.). Visual fluorescence signals were obtained using a fluorescence microscope (Olympus Corporation). The primary antibodies used were the following: adropin (1:200; cat. no. PA5-72781, Thermo Fisher Scientific, Inc.), CD68 (1:200, cat. no. ab53444, Abcam), inducible nitric oxide synthase (iNOS; 1:200, cat. no. ab3523, Abcam) and CD206 (1:200, cat. no. ab64693, Abcam).

*TUNEL fluorescence staining*. The paraffin-embedded sections were completely dewaxed with xylene, anhydrous ethanol, 90% ethanol, 75% ethanol and 50% ethanol, and incubated in protease K (cat. no. K1133A, ApexBio) at room temperature for 20 min. After the sections were slightly dried, they were incubated in equilibration buffer (cat. no. K1133, ApexBio) at room temperature for 20 min. An appropriate amount of TUNEL staining solution (TDT enzyme, dUTP, buffer mixed at a ratio of 1:5:50, cat. no. K1133, ApexBio) was added to cover the tissues. The sections were incubated in an incubator at 37˚C for 60 min. After PBS washes were applied, DAPI was applied for 10 min at room temperature. The sections were subsequently sealed with anti-fluorescence quenching sealing reagent, and photographed under a fluorescence microscope (Olympus Corporation).

*Enzyme-linked immunosorbent assay (ELISA)*. The serum samples were prepared for the ELISA of human adropin protein according to the manufacturer's instructions (Jiangsu Enzymatic Co., Ltd.; Lot: MM-50924H2). A standard curve was generated and the absorbance values were detected at 450 nm using a Synergy 2 Multi-Mode microplate reader (BioTek Instruments, Inc.).

*Western blot analysis*. The tissue proteins extracts were harvested from fresh pancreatic tissue using RIPA lysis buffer with protease and phosphatase inhibitors (cat. nos. G2002, G2006 and G2007, Wuhan Servicebio Technology Co., Ltd.). The protein concentration was quantified using the BCA method. Total proteins (30 $\mu$g) were separated by 10% SDS-PAGE and transferred to PVDF membranes. The PVDF membranes were blocked at room temperature for 20 min using a rapid sealing solution. The primary antibodies were used at 4˚C overnight, and the antibody included Adropin (1:1,000, cat. no. PA5-72781, Thermo Fisher Scientific, Inc.); GADPH (1:10,000; cat. no. AC001, ABclonal); peroxisome proliferator-activated receptor γ (PPARγ; 1:1,000, cat. no. bsm-52220R, BIOSS); p-PPARγ Ser112 (1:1,000, cat. no. bs-3737R, BIOSS); p-PPARγ Ser273 (1:1,000, cat. no. bs-2875R, BIOSS), caspase-3 (1:1,000, cat. no. YC0006, ImmunoWay Biotechnology Company) and PARP1 (1:1,000, cat. no. A0942, ABclonal). Visualization reagent (PL101, Shenzhen SunView technology Co., Ltd.) was used, and all blotted bands were analyzed using ImageJ 1.48 software (National Institutes of Health), and the intensity values were normalized to GADPH.

*Reverse transcription-quantitative PCR (RT-qPCR)*. Lung tissues were isolated using RNA isolater Total RNA Extraction Reagent (cat. no. RC112, Vazyme). The concentration of total RNA in the samples was determined using a spectrophotometer (Multiskan Go 1Drop, Thermo Fisher Scientific, Inc). cDNA was synthesized from 2,000 ng total RNA using the SweScript RT I First Strand cDNA Synthesis kit (cat. no. G3331, Wuhan Servicebio Technology Co., Ltd.). The cDNA was used for quantitative PCR (qPCR) using the 2X SYBR-Green qPCR Master Mix (cat. no. G3326, Wuhan Servicebio Technology Co., Ltd.) and the threshold cycle (CT) was determined using the ABI QuantStudio 5 (Thermo Fisher Scientific, Inc.). The PCR thermocycling: (95˚C 30 sec) x1 cycle; (95˚C 15 sec + 60˚C 10 sec + 72˚C 30 sec) x40 cycles. Relative gene expression was calculated based on normalization to β-actin. The primers and sequences used are presented in Table SI).

*Statistical analysis*. Data are presented as the mean ± standard deviation (SD) and GraphPad prism5.0 software (GraphPad Software, Inc.) was used for statistical analyses. An unpaired Student's t-test was utilized for comparisons between two groups. ANOVA was used to analyze multiple sets of data, and the Student-Newman-Keuls analysis was used to make pair-to-pair comparisons (three groups), and Tukey's multiple comparisons test was used to make pair-to-pair comparisons (four groups). A value of $P<0.05$ was considered to indicate a statistically significant difference.

## Results

*Adropin expression is lower in AP*. Clinical samples were collected from patients with AP and a mouse model of AP-ALI was constructed to explore the expression of adropin in the AP model. ELISA revealed that the average expression levels of adropin in the serum of patients with AP was lower than that of the healthy controls (551.8l vs. 362.8 pg/ml); however, there was no significant difference between the groups ($P=0.0622$, Fig. 1A). Moreover, the expression of serum adropin in the WT + L-Arg mouse group was significantly lower than in the WT + NS mouse group ($P<0.05$, Fig. 1B). In addition, serum α-amylase expression in the WT + L-Arg group was higher than that in the WT + NS group ($P<0.05$, Fig. 1C). H&E staining revealed evident intralobular and interlobular edema, diffuse acinar cell necrosis of the pancreas, inflammatory cell infiltration around the necrotic area, with the isolation of some acinar cells, nuclear contraction and notable inflammatory changes in the pancreatic tissues (Fig. 1F). RT-qPCR revealed that *Enho* mRNA expression in the WT + L-Arg group was higher than that in the WT + NS group ($P<0.05$, Fig. 1D), demonstrating that the expression of adropin in the WT + L-Arg group was lower than that in the WT + NS group; this was also shown by

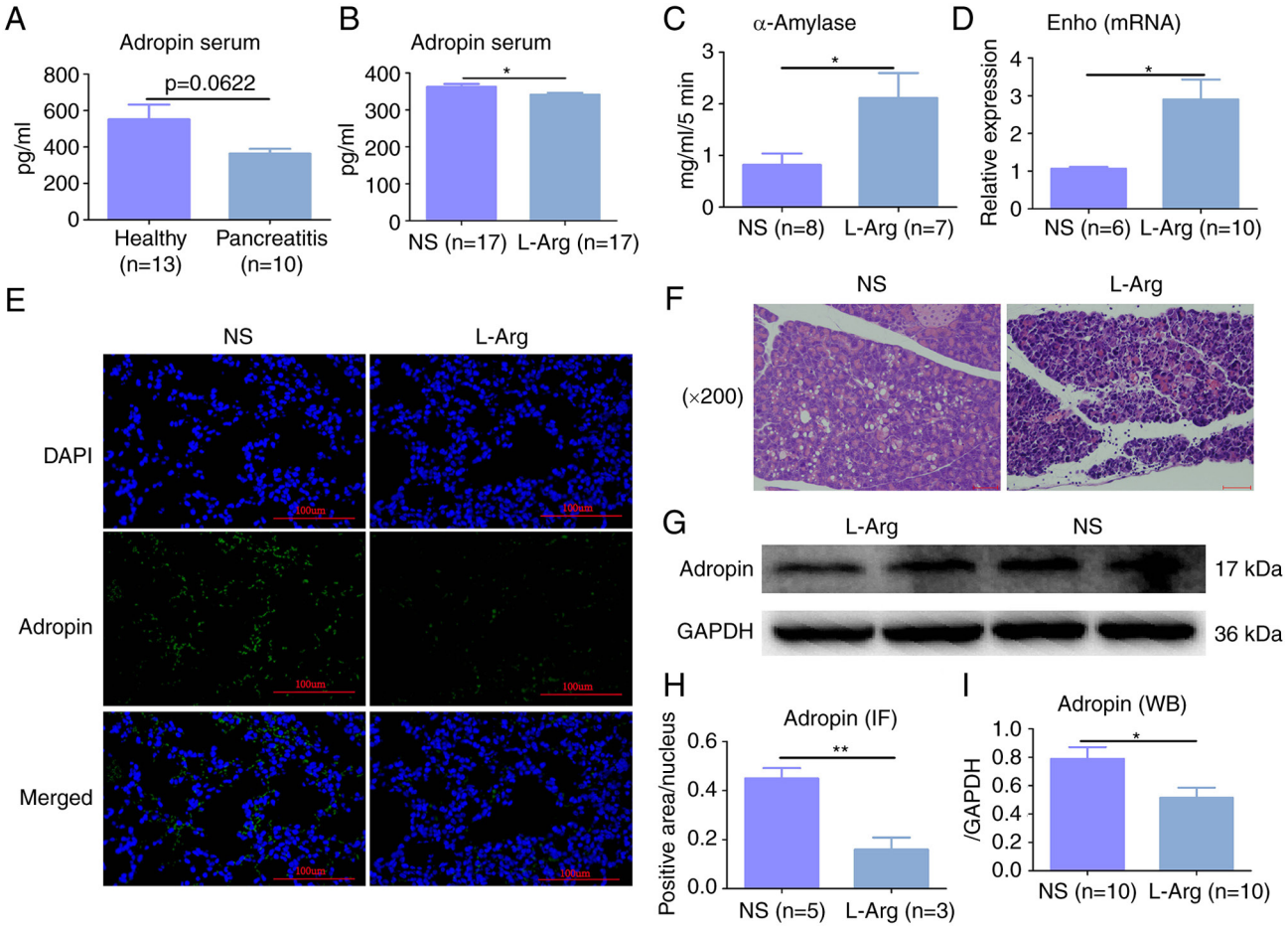


Figure 1. Adropin expression in AP-associated lung injury. (A) Adropin protein expression in serum in patients with AP. (B) Adropin protein expression in serum in the WT + L-Arg group. (C) Serum amylase level in the WT + L-Arg group. (D) *Enho* mRNA expression in the lung tissue in the WT + L-Arg group. (E) Adropin protein expression in lung tissue in the WT + L-Arg group determined using immunofluorescence. (F) Hematoxylin and eosin staining of pancreatic tissue in the WT + L-Arg group. (G) The adropin protein expression in lung tissue was measured using western blotting. (H) Quantitative analysis of adropin expression determined using immunofluorescence in panel E. (I) Quantitative analysis of the western blots in panel G. $^{*}$P<0.05 and $^{**}$P<0.01. AP, acute pancreatitis; L-Arg, L-arginine; NS, normal saline; Enho, energy homeostasis-associated gene.

both immunofluorescence and western blot analysis (P<0.05, Fig. 1E, G, H and I).

*Animal model of Adro-KO and L-Arg-induced AP exhibits severe AP-ALI.* An Adro-KO mouse model and a model of AP were constructed, and the degree of lung injury was evaluated using immunohistochemistry and western blot analysis. Masson's staining revealed that the level of fibrosis in the Adro-KO + L-Arg group was higher than that in the WT + L-Arg group (P<0.05, Fig. 2A and E). Immunohistochemistry revealed that the positive intensity of TGF-β in the Adro-KO + L-Arg group was higher than that in the Adro-KO + NS and WT + L-Arg groups, while the WT + L-Arg group demonstrated higher levels of TGF-β than the WT + NS group (P<0.05, Fig. 2A and F). The positive intensity of CD68 in the Adro-KO + L-Arg group was higher than that in the Adro-KO + NS group, while the intensity of CD68 in the WT + L-Arg group was higher than that in the WT + NS group (P<0.05, Fig. 2A and G). Western blot analysis demonstrated that the protein expression of caspase-3 and PARP1 in the lung tissues collected from the mice in the Adro-KO + L-Arg group was higher than that in the WT + L-Arg group (P<0.05, Fig. 2B, H and I). TUNEL staining similarly revealed that the level of apoptosis in the lung tissues from the mice in the Adro-KO + L-Arg group was higher than that in the WT + L-Arg group (P<0.05, Fig. 2C and D).

*Adro-KO and L-Arg lead to excessive M1 macrophage polarization.* In addition, using the established models of Adro-KO AP, the phosphorylation of PPARγ and the polarization of macrophages were evaluated using immunofluorescence and western blot analysis. Western blot analysis revealed that the protein expression of PPARγ in the lung tissues of mice from the Adro-KO + L-Arg group was lower than that in the WT + L-Arg group (P<0.05, Fig. 3A and J). The phosphorylation levels of PPARγ Ser112 and PPARγ Ser273 in the lungs of mice in the Adro-KO + L-Arg group were higher than those in the WT + L-Arg group (P<0.05, Fig. 3A, K and L). The results also indicated that the co-expression of iNOS and CD68 in the lung tissues from the WT + L-Arg group was higher than that in the WT + NS group (P<0.05, Fig. 3B and H). The co-expression of CD206 and CD68 in the lung tissues from the WT + L-Arg group was lower than that in the WT + NS group (P<0.05, Fig. 3C and I). In addition, the results demonstrated that the mRNA expression of iNOS and CD86 in the lung tissue from the Adro-KO + L-Arg group was higher than that in the

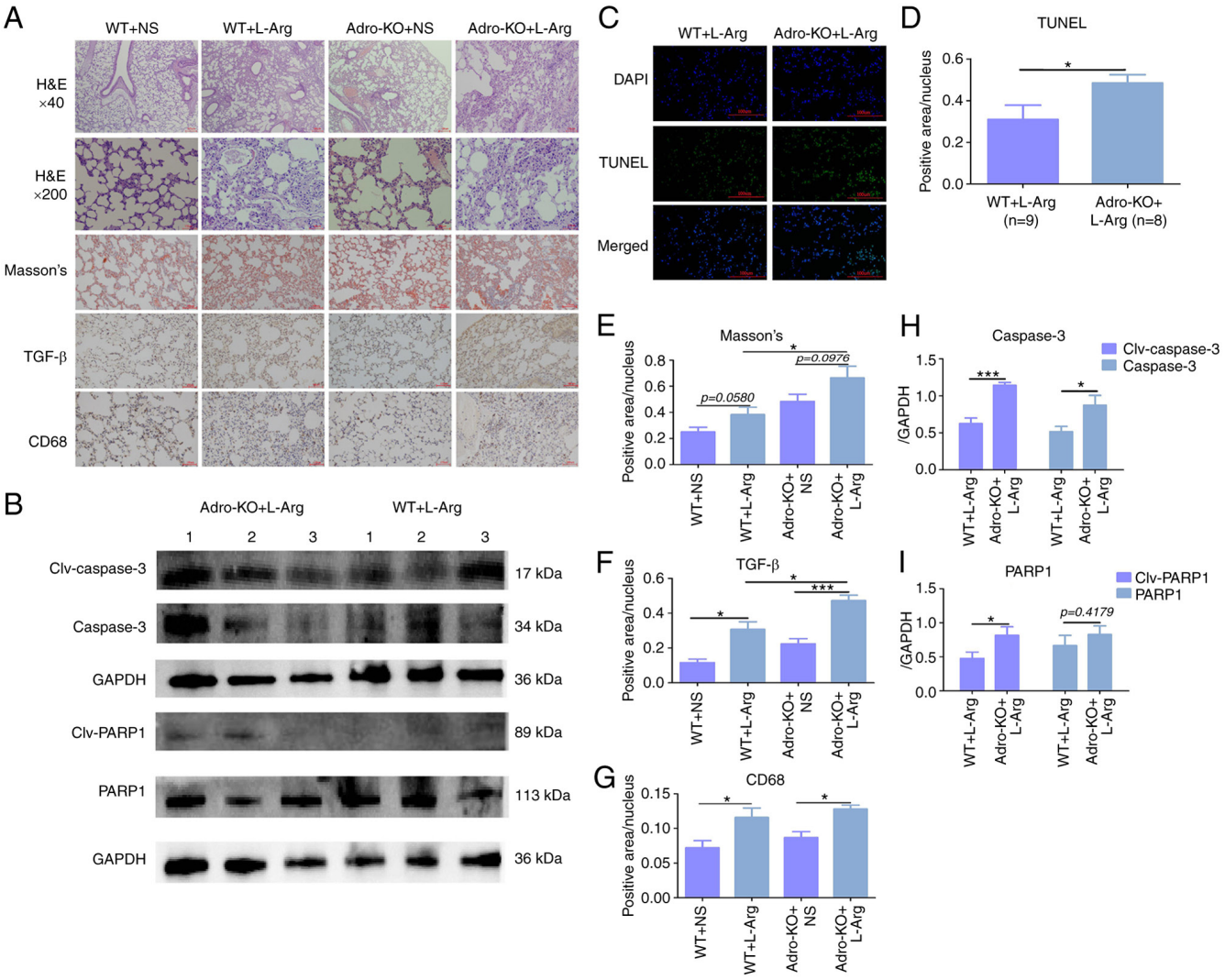


Figure 2. Results reveal severe acute pancreatitis-associated lung injury in the Adro-KO + L-Arg group. (A) H&E, Masson's staining and immunohistochemistry of lung tissue in the Adro-KO + L-Arg group. (B) Western blot analysis of lung tissue in the Adro-KO + L-Arg group. (C) TUNEL staining of lung tissue in the Adro-KO + L-Arg group. (D) Quantitative analysis of TUNEL staining shown in panel C (n≥8). (E) Quantitative analysis of Masson's staining shown in panel A (n≥7). (F) Quantitative analysis of immunohistochemistry (TGF-β; n≥3). (G) Quantitative analysis of immunohistochemistry (CD68; n≥5). (H) Quantitative analysis of the western blots (caspase-3; n=9). (I) Quantitative analysis of the western blots (PARP1; n=9). *P<0.05 and ***P<0.001. L-Arg, L-arginine; H&E, hematoxylin and eosin; Adro-KO, adropin knockout; NS, normal saline.

WT + L-Arg group (P<0.05, Fig. 3D and E). It was also found that the mRNA levels of CD163 and arginase 1 (Arg-1) in the lung tissues from the Adro-KO + L-Arg group were lower than those in the WT + L-Arg group (P<0.05, Fig. 3F and G).

*Adropin exogenous supplement attenuates AP-ALI*. Rescue experiments were then performed using exogenous adropin and the protective effect of adropin was examined in animal models of AP. Immunohistochemistry revealed that the positive intensity of PARP1 and caspase-3 in lung tissues from the Adro-KO + L-Arg + Adro$^{(34-76)}$ group was lower than that in the Adro-KO + L-Arg group (P<0.05, Fig. 4A, F and G). There were no significant differences in the protein expression of MPO and CD68 in the lung tissues between the Adro-KO + L-Arg+Adro$^{(34-76)}$ and Adro-KO + L-Arg groups (P<0.05, Fig. 4A, D and E). The results also demonstrated that the protein expression levels of cleaved caspase-3 and cleaved PARP1 in the lung tissues from the Adro-KO + L-Arg + Adro$^{(34-76)}$ group were lower than those in the Adro-KO + L-Arg group (P<0.05, Fig. 4B, H and I). Of note, the protein expression levels of caspase-3 and PARP1 in the lung tissues from the Adro-KO + L-Arg + Adro$^{(34-76)}$ and Adro-KO + L-Arg groups exhibited no significant differences (Fig. 4B, H and I). These results also indicated that the intensity of TUNEL staining in the lung tissue obtained from the Adro-KO + L-Arg + Adro$^{(34-76)}$ group was lower than that in the Adro-KO + L-Arg group (P<0.05, Fig. 4C and J).

*Adropin exogenous supplement induceS M2 macrophage polarization*. Rescue experiments were then performed using exogenous adropin to further explore the effects of exogenous adropin on PPARγ phosphorylation and macrophage polarization. Western blot analysis revealed that the protein expression levels of PPARγ, PPARγ Ser112 and PPARγ Ser273 in the Adro-KO + L-Arg + Adro$^{(34-76)}$ group were higher than those in the Adro-KO + L-Arg group (P<0.05, Fig. 5A and B). Immunofluorescence revealed that the co-expression of iNOS and CD68 in the lung tissues from the Adro-KO + L-Arg + Adro$^{(34-76)}$ group was lower than that in the Adro-KO + L-Arg

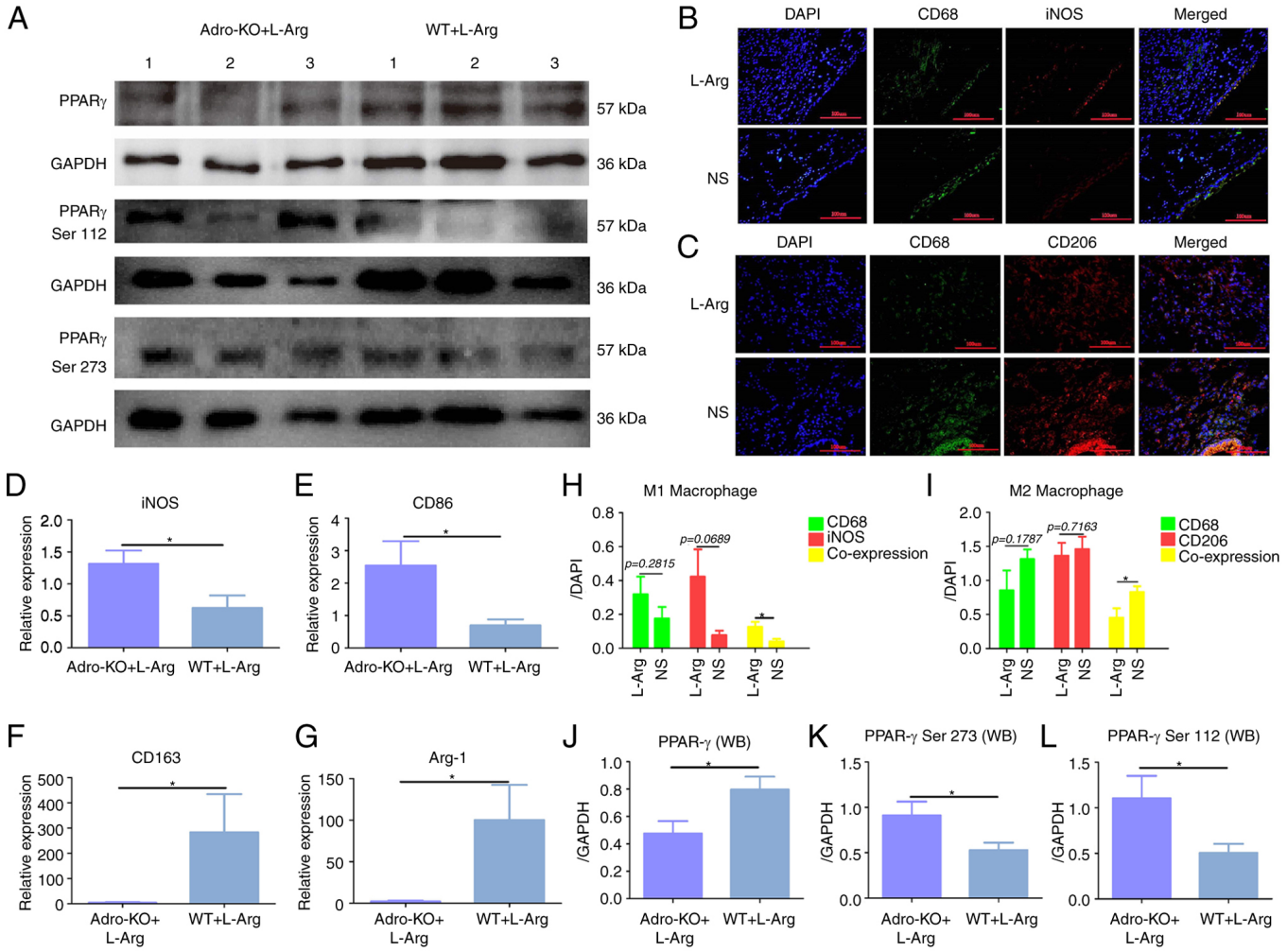


Figure 3. Excessive M1 macrophage polarization is observed in the Adro-KO + L-Arg group. (A) Western blot analysis of lung tissue form the Adro-KO + L-Arg group. (B) Co-expression of CD68 and iNOS in lung tissue in L-Arg group determined using immunofluorescence. (C) Co-expression of CD68 and CD206 of lung tissue in the L-Arg group determined using immunofluorescence. (D) iNOS mRNA level in lung tissue from the Adro-KO + L-Arg group (n≥8). (E) CD68 mRNA level in lung tissue from the Adro-KO + L-Arg group (n≥7). (F) CD163 mRNA level in lung tissue from the Adro-KO + L-Arg group (n≥8). (G) Arg-1 mRNA level in lung tissue from the Adro-KO + L-Arg group (n≥8). (H) Quantitative analysis of immunofluorescence (CD68 + iNOS) staining (n≥5). (I) Quantitative analysis of immunofluorescence (CD68; CD206) staining in macrophages (n≥9). (J) Quantitative analysis of the western blots (PPARγ; n≥6); (K) Quantitative analysis of the western blots (PPARγ Ser273; n≥6). (L) Quantitative analysis of the western blots (PPARγ Ser112; n≥6). *P<0.05. L-Arg, L-arginine; NS, normal saline; Adro-KO, adropin knockout; iNOS, inducible nitric oxide synthase.

group (P<0.05, Fig. 5C and E-G). Furthermore, the results indicated that the co-expression of CD206 and CD68 in the lung tissues from the Adro-KO + L-Arg + Adro$^{(34-76)}$ group was higher than that in the Adro-KO + L-Arg group (P<0.05, Fig. 5D and H-J). In addition, RT-qPCR demonstrated that the mRNA expression of CD163 and Arg-1 in the Adro-KO + L-Arg + Adro$^{(34-76)}$ group was higher than that in the Adro-KO + L-Arg group (P<0.05, Fig. 5K and L). Comparatively, the mRNA expression of iNOS and CD86 in the Adro-KO + L-Arg + Adro$^{(34-76)}$ group and the Adro-KO + L -Arg group exhibited no significant difference (P>0.05, Fig. 5M and N).

## Discussion

The results of the present study suggested that adropin may play a crucial role in the progression of AP-ALI. In contrast to the decreased protein expression of adropin in lung and serum in AP, the increased mRNA expression of *Enho* was found in lung tissue in AP, suggesting that the low expression of adropin may be related to increased degradation. An animal model of Adro-KO AP was established, observing that the level of apoptosis in lung tissue in the Adro-KO group was significantly higher than that in the NS group. It was also found that the expression of PPAR-γ in Adro-KO group was downregulated and that M1 macrophage polarization was increased. Based on these findings, it was hypothesized that the decreased expression of adropin could exacerbate AP-ALI by affecting the function of PPAR-γ protein and the polarization of pulmonary macrophages. To further examine this hypothesis, adropin rescue experiments were conducted, discovering that adropin exogenous supplementation resulted in a lower level of lung apoptosis in the Adro-KO + L-Arg + Adro$^{(34-76)}$ group compared with the Adro-KO + L-Arg group. At the same time, adropin$^{(34-76)}$ was evaluated in an adropin-KO model, demonstrating an increased expression of PPAR-γ, a decrease in M1 macrophage polarization and an increased M2 macrophage polarization. Rescue experiments also supported the aforementioned hypothesis. In summary, the results

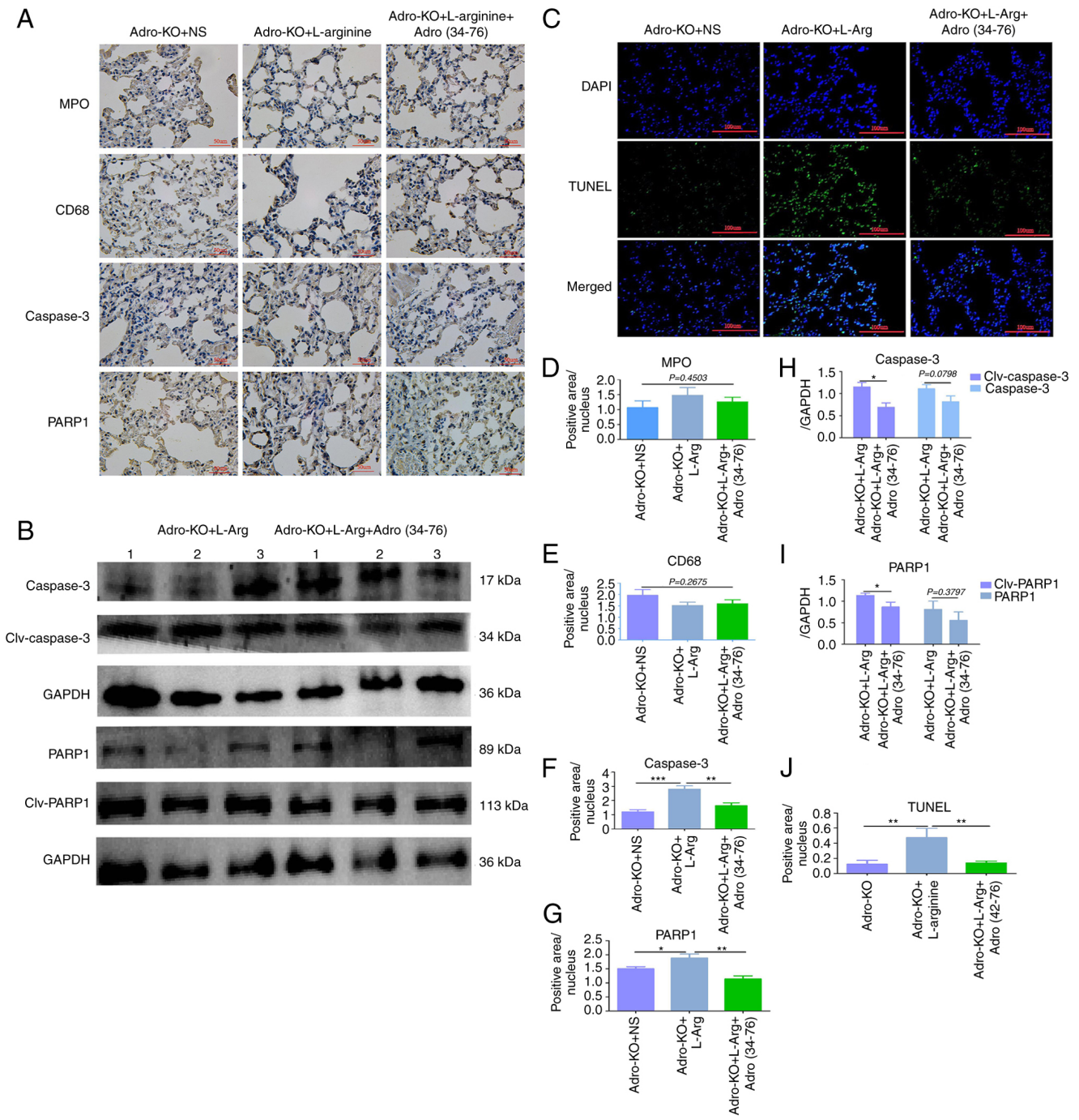


Figure 4. Adropin exogenous supplement attenuates severe acute pancreatitis-associated lung injury. (A) Immunohistochemistry of lung tissue from the Adroko + L-Arg + Adro$^{(34-76)}$group. (B) Western blot analysis of lung tissue from the Adro-KO + L-Arg + Adro$^{(34-76)}$ group. (C) TUNEL staining of lung tissue from the Adro-KO + L-Arg + Adro$^{(34-76)}$ group. (D) Quantitative analysis of immunohistochemistry for MPO (n≥4). (E) Quantitative analysis of immunohistochemistry for CD68 (n≥4). (F) Quantitative analysis of immunohistochemistry for caspase-3 (n≥5). (G) Quantitative analysis of immunohistochemistry for PARP1 (n≥3). (H) Quantitative analysis of the western blots (caspase-3) (n≥5). (I) Quantitative analysis of the western blots (PARP1) (n≥6). (J) Quantitative analysis of TUNEL staining from panel C (n≥5). $^{*}$P<0.05, $^{**}$P<0.01 and $^{***}$P<0.001. L-Arg, L-arginine; Adro-KO, adropin knockout; NS, normal saline; MPO, myeloperoxidase.

preliminarily demonstrated that adropin regulated AP-ALI by affecting the protein function of PPAR-γ and the polarization of lung macrophages.

The results of the present study demonstrated that adropin expression in lung tissue and serum in AP-ALI models ws decreased, supporting the likelihood of its involvement in the progression of AP-ALI. Adropin can regulate renal function and inflammatory responses, exerting a protective effect on the progression of systemic inflammation and renal failure (15). Adropin has been shown to inhibit inflammation by reducing the levels of pro-inflammatory cytokines and IL-6 in tissues (16). Additionally, adropin has been found to improve non-alcoholic steatohepatitis by inhibiting the activation of the NLRP3 inflammasome (17). Plasma adropin concentrations have been shown to be negatively associated with plasma biomarkers of systemic inflammation, suggesting that adropin may play an anti-inflammatory role in obstructive sleep apnea (18). Combined with the findings of the present study and those reported above, it was

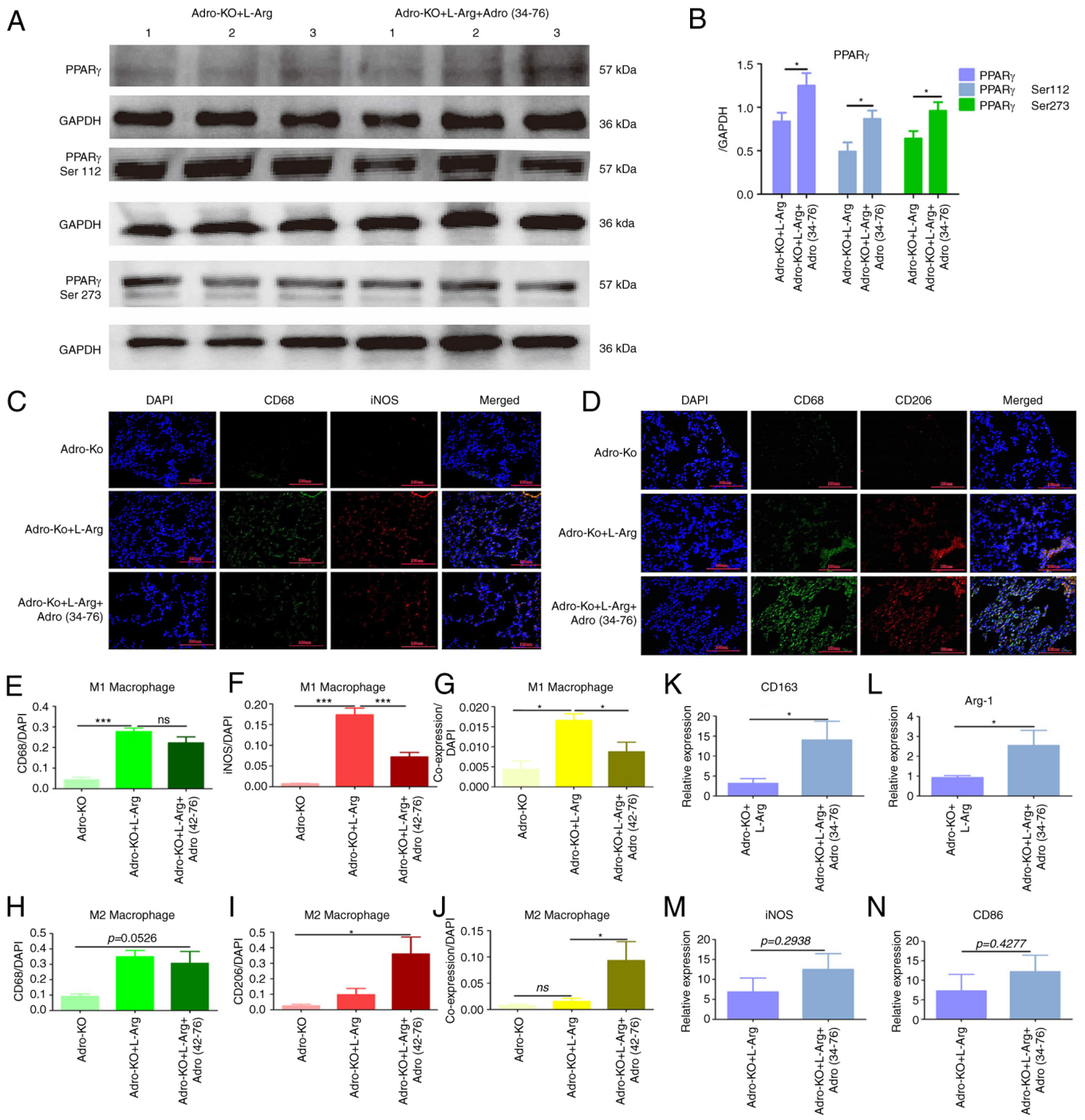


Figure 5. Adropin exogenous supplement induces M2 macrophage polarization. (A) Western blot analysis of lung tissue from the Adro-KO + L-Arg + Adro$^{(34-76)}$ group. (B) Quantitative analysis of the western blots (PPARγ, PPARγ Ser112, PPARγ Ser273) (n≥5). (C) Co-expression of CD68 and iNOS in lung tissue from the Adro-KO + L-Arg+Adro$^{(34-76)}$ group. (D) Co-expression of CD68 and iNOS in lung tissue from the Adro-KO + L-Arg + Adro$^{(34-76)}$ group. (E) Ratio of CD68/DAPI of lung in Adro-KO+ L-Arg+Adro$^{(34-76)}$ group(n≥3); (F) The ratio of iNOS/DAPI in lung tissue from the Adro-KO + L-Arg + Adro$^{(34-76)}$ group (n≥3). (G) Ratio of iNOS/CD68 in lung tissue from the Adro-KO + L-Arg + Adro$^{(34-76)}$ group (n≥3). (H) Ratio of CD68/DAPI in lung tissue from the Adro-KO + L-Arg + Adro$^{(34-76)}$ group (n≥3). (I) Ratio of CD206/DAPI in lung tissue from the Adro-KO + L-Arg + Adro$^{(34-76)}$ group (n≥3). (J) Ratio of CD206/CD68 in lung tissue from the Adro-KO + L-Arg + Adro$^{(34-76)}$ group (n≥3). (K) CD163 mRNA level in lung tissue from the Adro-KO + L-Arg + Adro$^{(34-76)}$ group (n≥6). (L) Arg-1 mRNA level in lung tissue from the Adro-KO + L-Arg + Adro$^{(34-76)}$ group (n≥6). (M) iNOS mRNA level in lung tissue from the Adro-KO + L-Arg + Adro$^{(34-76)}$ group (n≥6). (N) CD86 mRNA level level in lung tissue from the Adro-KO + L-Arg + Adro$^{(34-76)}$ group (n≥6). $^{*}$P<0.05 and $^{***}$P<0.001. L-Arg, L-arginine; Adro-KO, adropin knockout; NS, normal saline; iNOS, inducible nitric oxide synthase; Arg-1, arginase 1.

hypothesized that the decreased expression of adropin in lung and serum may exacerbate immune disorders and inflammatory damage in AP-ALI models.

The present study found an increased number of CD68-positive macrophages in the lungs of mice with AP-ALI. At the same time, it was found that in the Adro-KO + L-Arg group, the mRNA expression levels of CD206 and Arg-1 were decreased, while the mRNA expression levels of iNOS and CD86 were increased. Moreover, the results of immunofluorescence staining demonstrated that the expression of

CD206 in the Adro-KO + L-Arg group decreased, while the expression of iNOS increased, suggesting that the absence of adropin was associated with macrophage M1 polarization. The expression of PPARγ was downregulated, and the phosphorylation of Ser112 and Ser273 was increased. The results of the present study are consistent with those reported previously in the literature. For example, adropin has been shown to regulate macrophage polarization by regulating the expression of PPAR-γ, a gene related to fatty acid metabolism (6). Adropin has also been found to transfer the phenotype to the anti-inflammatory M2 rather than pro-inflammatory M1 during monocyte differentiation into macrophages through the upregulation of PPAR-γ (19). The long-term administration of adropin in Apoe$^{-/-}$ mice has been shown to reduce the development of aortic atherosclerotic lesions, mononuclear/macrophage infiltration and smooth muscle cell content in plaque (20). The upregulation of PPAR-γ expression and induced PPAR-γ dephosphorylation at the Ser112 site plays an anti-inflammatory role (21). The inhibition of the phosphorylation of PPAR-γ at the Ser112 site in macrophages activates PPAR-γ, inducing the expression of ATP-binding box transporter A1 and producing anti-atherosclerotic effects (22). It was hypothesized that Adro-KO would lead to an increased phosphorylation of PPARγ at Ser112 and Ser273 sites, and inhibit PPARγ function, resulting in an increased M1 type of macrophages in lung tissue.

The results of the present study revealed that the proportion of M1 macrophages increased and lung tissue damage increased in the Adro-KO + L-Arg model. Moreover, it was found that exogenous adropin improved M2 macrophage polarization and reduced lung inflammatory damage through rescue experiments. The results of pathological molecular experiments revealed that the intensity of TGF-β and Masson's staining in the Adro-KO + L-Arg group was higher than that in the WT + L-Arg group. The results of western blot analysis demonstrated that the expression of cleaved caspse-3 and cleaed PARP1 was decreased in the Adro-KO + L-Arg + Adro$^{(34-76)}$ group, indicating that adropin exerted an anti-apoptotic effect on AP-ALI. It has been found that alveolar macrophage death plays a crucial role in the progression of pneumonia by affecting other immune cell populations in the lungs (23). A recent study demonstrated that macrophages were key regulatory factors in the pathogenesis of acute lung injury/acute respiratory distress syndrome. As such, regulating macrophage polarization may improve the prognosis of acute lung injury (24). Macrophages are involved in the development and progression of acute lung injury through the secretion of inflammatory cytokines/chemokines and the activation of transcription factors in the pathogenesis of inflammatory lung diseases (25). The activation of PPAR-γ in alveolar macrophages demonstrates a protective effect against LPS-induced acute lung injury in mice (26). Macrophages play a critical role in the regulation of lung inflammatory lung injury. Combined with our result and the literature above (6,26). Adropin may reduce inflammatory injury by regulating the polarization of lung macrophages, identifying a potential therapeutic target for lung injury in acute pancreatitis.

One limitation of the present study is the lack of high-throughput protein sequencing to construct a relatively complete adropin-related signaling pathway. The authors hope to perfrom such an investigation in the future. The present study may have also benefited from flow cytometry for the serum neutralization of lung macrophages. Finally, the dose selection in the rescue experiment was based on reference literature instead of a concentration gradient. Due to the lack of an adropin$^{(34-76)}$ gradient, it could not be ruled out whether some results were attributable to an insufficient dose or functional limitations of adropin$^{(34-76)}$. In the future, further studies are required to explore the immune regulatory effects of adropin on acute pancreatitis. The key questions remaining to be answered include: i) Whether adropin regulates macrophage polarization and the molecular mechanisms in AP-ALI; ii) the regulatory effects of adropin expression in the occurrence and development of AP-ALI.

In conclusion, the present study demonstrates that the decreased expression of adropin in lung tissue and serum may aggravate immune disorders and inflammatory injury in AP. The knockout of adropin resulted in the increased expression of PPARγ at Ser112 and Ser273, inhibiting PPARγ function and resulting in increased M1 macrophage in lung tissue. Exogenous adropin alleviated inflammatory damage by regulating the polarization of lung macrophages. This finding may be leveraged to improve AP-associated pneumonia and may markedly improve the prognosis of patients with AP.

**Acknowledgements**

Not applicable.

**Funding**

The present study was funded by grants from the Sailing Foundation of Fujian Medical University (no. 2022QH2033) and the Natural Science Foundation of Fujian Province (no. 2020J01961).

**Availability of data and materials**

The datasets used and/or analyzed during the current study are available from the corresponding author on reasonable request.

**Authors' contributions**

YC and SW planned the study. FD and FG conceived and designed the study. FD and GL performed the collection of the samples. FD and ZZ performed the immunohistochemistry experiment. GL and YH performed the analyses of expression levels. FD and GL confirm the authenticity of all the raw data. All the authors carefully reviewed the manuscript and all authors have read and approved the final version.

**Ethics approval and consent to participate**

All patients provided informed consent for excess specimens to be used for research purposes and all protocols employed in the study were approved by the Medical Ethics Committee of The First Affiliated Hospital of Fujian Medical University [MTCA, ECFAH of FMU(2015) 084-1]. All animal experiments complied with the National Institutes of Health guidelines for the care and used of laboratory animals, and

the protocol was approved by the Ethics Committee of Fujian Medical University (IACUC FJMU 2022-0428).

### Patient consent for publication

Not applicable.

### Competing interests

The authors declare that have no competing interests.

### References


1. Petrov MS and Yadav D: Global epidemiology and holistic prevention of pancreatitis. Nat Rev Gastroenterol Hepatol 16: 175-184, 2019.
2. Liu W, Du JJ, Li ZH, Zhang XY and Zuo HD: Liver injury associated with acute pancreatitis: The current status of clinical evaluation and involved mechanisms. World J Clin Cases 9: 10418-10429, 2021.
3. Cao C, Yin C, Shou S, Wang J, Yu L, Li X and Chai Y: Ulinastatin protects against LPS-induced acute lung injury by attenuating TLR4/NF-κB pathway activation and reducing inflammatory mediators. Shock 50: 595-605, 2018.
4. Liu D, Wen L, Wang Z, Hai Y, Yang D, Zhang Y, Bai M, Song B and Wang Y: The Mechanism of lung and intestinal injury in acute pancreatitis: A review. Front Med (Lausanne) 9: 904078, 2022.
5. Huai JP, Sun XC, Chen MJ, Jin Y, Ye XH, Wu JS and Huang ZM: Melatonin attenuates acute pancreatitis-associated lung injury in rats by modulating interleukin 22. World J Gastroenterol 18: 5122-5128, 2012.
6. Zhang S, Chen Q, Lin X, Chen M and Liu Q: A review of adropin as the medium of dialogue between energy regulation and immune regulation. Oxid Med Cell Longev 2020: 3947806, 2020.
7. Algul S and Ozcelik O: Evaluating the energy regulatory hormones of nesfatin-1, irisin, adropin and preptin in multiple sclerosis. Mult Scler Relat Disord 68: 104221, 2022.
8. Dodd WS, Patel D, Lucke-Wold B, Hosaka K, Chalouhi N and Hoh BL: Adropin decreases endothelial monolayer permeability after cell-free hemoglobin exposure and reduces MCP-1-induced macrophage transmigration. Biochem Biophys Res Commun 582: 105-110, 2021.
9. Chen S, Zeng K, Liu QC, Guo Z, Zhang S, Chen XR, Lin JH, Wen JP, Zhao CF, Lin XH and Gao F: Adropin deficiency worsens HFD-induced metabolic defects. Cell Death Dis 8: e3008, 2017.
10. Gao F, Fang J, Chen F, Wang C, Chen S, Zhang S, Lv X, Zhang J, He Q, Weng S, *et al*: Enho mutations causing low adropin: A possible pathomechanism of MPO-ANCA associated lung injury. EBioMedicine 9: 324-335, 2016.
11. Shen J, Wan R, Hu G, Wang F, Shen J and Wang X: Involvement of thrombopoietin in acinar cell necrosis in L-arginine-induced acute pancreatitis in mice. Cytokine 60: 294-301, 2012.
12. Gao S, Ghoshal S, Zhang L, Stevens JR, McCommis KS, Finck BN, Lopaschuk GD and Butler AA: The peptide hormone adropin regulates signal transduction pathways controlling hepatic glucose metabolism in a mouse model of diet-induced obesity. J Biol Chem 294: 13366-13377, 2019.
13. Gao S, McMillan RP, Zhu Q, Lopaschuk GD, Hulver MW and Butler AA: Therapeutic effects of adropin on glucose tolerance and substrate utilization in diet-induced obese mice with insulin resistance. Mol Metab 4: 310-324, 2015.
14. Mikawa K, Nishina K, Takao Y and Obara H: ONO-1714, a nitric oxide synthase inhibitor, attenuates endotoxin-induced acute lung injury in rabbits. Anesth Analg 97: 1751-1755, 2003.
15. Memi G and Yazgan B: Adropin and spexin hormones regulate the systemic inflammation in adenine-induced chronic kidney failure in rat. Chin J Physiol 64: 194-201, 2021.
16. Ali II, D'Souza C, Singh J and Adeghate E: Adropin's role in energy homeostasis and metabolic disorders. Int J Mol Sci 23: 8318, 2022.
17. Yang W, Liu L, Wei Y, Fang C, Liu S, Zhou F, Li Y, Zhao G, Guo Z, Luo Y and Li L: Exercise suppresses NLRP3 inflammasome activation in mice with diet-induced NASH: A plausible role of adropin. Lab Invest 101: 369-380, 2021.
18. Bozic J, Borovac JA, Galic T, Kurir TT, Supe-Domic D and Dogas Z: Adropin and inflammation biomarker levels in male patients with obstructive sleep apnea: A link with glucose metabolism and sleep parameters. J Clin Sleep Med 14: 1109-1118, 2018.
19. Sato K, Yamashita T, Shirai R, Shibata K, Okano T, Yamaguchi M, Mori Y, Hirano T and Watanabe T: Adropin contributes to anti-atherosclerosis by suppressing monocyte-endothelial cell adhesion and smooth muscle cell proliferation. Int J Mol Sci 19: 1293, 2018.
20. Li L and Xie W: LncRNA HDAC11-AS1 suppresses atherosclerosis by inhibiting HDAC11-mediated adropin histone deacetylation. J Cardiovasc Transl Res 15: 1256-1269, 2022.
21. Yu T, Gao M, Yang P, Liu D, Wang D, Song F, Zhang X and Liu Y: Insulin promotes macrophage phenotype transition through PI3K/Akt and PPAR-γ signaling during diabetic wound healing. J Cell Physiol 234: 4217-4231, 2019.
22. Ishii N, Matsumura T, Kinoshita H, Fukuda K, Motoshima H, Senokuchi T, Nakao S, Tsutsumi A, Kim-Mitsuyama S, Kawada T, *et al*: Nifedipine induces peroxisome proliferator-activated receptor-gamma activation in macrophages and suppresses the progression of atherosclerosis in apolipoprotein E-deficient mice. Arterioscler Thromb Vasc Biol 30: 1598-1605, 2010.
23. Fan EKY and Fan J: Regulation of alveolar macrophage death in acute lung inflammation. Respir Res 19: 50, 2018.
24. Chen X, Tang J, Shuai W, Meng J, Feng J and Han Z: Macrophage polarization and its role in the pathogenesis of acute lung injury/acute respiratory distress syndrome. Inflamm Res 69: 883-895, 2020.
25. Lee JW, Chun W, Lee HJ, Min JH, Kim SM, Seo JY, Ahn KS and Oh SR: The role of macrophages in the development of acute and chronic inflammatory lung diseases. Cells 10: 897, 2021.
26. Shen Y, Sun Z and Guo X: Citral inhibits lipopolysaccharide-induced acute lung injury by activating PPAR-γ. Eur J Pharmacol 747: 45-51, 2015.